Quantum dynamical study of the O (D 1) + H Cl reaction employing three electronic state potential energy surfaces

Huan Yang, Ke-Li Han, Shinkoh Nanbu, Hiroki Nakamura, Gabriel G. Balint-Kurti, Hong Zhang, Sean C. Smith, and Marlies Hankel

Citation: The Journal of Chemical Physics **128**, 014308 (2008); doi: 10.1063/1.2813414
View online: http://dx.doi.org/10.1063/1.2813414
View Table of Contents: http://scitation.aip.org/content/aip/journal/jcp/128/1?ver=pdfcov
Published by the AIP Publishing

Quantum dynamical study of the O(^1D)+HCl reaction employing three electronic state potential energy surfaces

Huan Yang and Ke-Li Han
State Key Laboratory of Molecular Reaction Dynamics, Dalian Institute of Chemical Physics, Chinese Academy of Sciences, Dalian 116023, People's Republic of China

Shinkoh Nanbu
Research Institute for Information Technology, Kyushu University, 6-10-1 Hakozaki Higashi-ku Fukuoka 812-8581, Japan

Hiroki Nakamura
Institute for Molecular Science, Myodaiji, Okazaki 444-8585, Japan

Gabriel G. Balint-Kurti
School of Chemistry, University of Bristol, Bristol BS8 1TS, United Kingdom

Hong Zhang, Sean C. Smith, and Marlies Hankel[a)]
Centre for Computational Molecular Science, Australian Institute for Bioengineering and Nanotechnology, The University of Queensland, Queensland 4072, Australia

(Received 5 October 2007; accepted 24 October 2007; published online 7 January 2008)

Quantum dynamical calculations are reported for the title reaction, for both product arrangement channels and using potential energy surfaces corresponding to the three electronic states, $1\,^1A'$, $2\,^1A'$, and $1\,^1A''$, which correlate with both reactants and products. The calculations have been performed for $J=0$ using the time-dependent real wavepacket approach by Gray and Balint-Kurti [J. Chem. Phys. **108**, 950 (1998)]. Reaction probabilities for both product arrangement channels on all three potential energy surfaces are presented for total energies between 0.1 and 1.1 eV. Product vibrational state distributions at two total energies, 0.522 and 0.722 eV, are also presented for both channels and all three electronic states. Product rotational quantum state distributions are presented for both product arrangement channels and all three electronic states for the first six product vibrational states. © *2008 American Institute of Physics*. [DOI: 10.1063/1.2813414]

I. INTRODUCTION

The reaction of electronically excited oxygen with hydrochloric acid has been a focus of several experimental[1–9] and theoretical studies.[10–33] The reaction plays an important role in the modeling of atmospheric chemistry and presents an interesting system for the study of fundamental dynamics. For O(^1D)+HCl, the following two reaction channels compete:

$$\mathrm{O}(^1D) + \mathrm{HCl} \rightarrow \mathrm{OH} + \mathrm{Cl}, \tag{1}$$

$$\rightarrow \mathrm{OCl} + \mathrm{H}. \tag{2}$$

Five electronic states correlate with the reactants, of which three, $1\,^1A'$, $1\,^1A''$, and $2\,^1A'$, also correlate with the products (for simplicity, we will omit the singlet superscript). Several potential energy surfaces (PESs) for the ground state are available.[10,11,19,23,27] Most previous theoretical investigations have been carried out considering only the ground state. Recently, Nanbu *et al.*[27] published new global PESs for all three electronic states. They performed time-independent quantum dynamical calculations on all three surfaces.[28,29] In the current paper, we employ a new improved PESs by Nanbu,[34] including again all three electronic states. 1761 points for each PES have been added in the vicinity of the HOCl equilibrium to refine the first generation PESs. The ground state, $1A'$, has two deep wells in bent geometries corresponding to the stable HOCl and HClO molecules. Taking the zero of energy to be the asymptotic energy of the reactants, the well depth of HOCl is 4.4 eV, (measured from this zero of energy), while that of HClO is 1.99 eV. The excess energy for the OH+Cl formation is 1.92 eV, while that of OCl+H is 0.02 eV. The two excited state PESs have no minima. On the $1A''$ state, the barrier to form OH+Cl products is only about 0.09 eV, while the one to form OCl +H is quite high at 0.62 eV. The $2A'$ state correlates only with the OH+Cl products possessing a barrier of about 0.28 eV for this process. These minima and transition state energies are only slightly different from those reported for the first generation PESs,[27] except that the barrier on the $1A''$ state to form OCl+H products is 0.7 eV on the first generation PES and the HClO well depth is 1.94 eV.

Calculations employing the time-dependent real wavepacket method[35] have been performed to calculate state-to-state reaction probabilities for total angular momentum $J=0$. Calculations for both product arrangement channels employing all three electronic state PESs have been carried out.

[a)]Author to whom correspondence should be addressed. Electronic mail: m.hankel@uq.edu.au.

TABLE I. Grid and initial condition details for the calculations. All quantities are in a.u. unless stated otherwise.

	OH+Cl			OCl+H	
Variable	$1A'$	$1A''$	$2A'$	$1A'$	$1A''$
Scattering coordinate (R) range	0–15	0.5–15	0.5–15	0.5–15	0.5–15
Number of grid points in R	399	299	299	209	299
Internal coordinate (r) range	0–13	0.5–15	0.5–15	0.5–15	0.5–15
Number of grid points in r	272	299	299	299	299
Number of angular grid points	100	120	120	143	120
Absorption region length in R (r)	4 (2)	4 (4.5)	4 (4.5)	3 (2.5)	4 (4.5)
Absorption strength in R (r)	0.1 (0.1)	0.1 (0.1)	0.1 (0.1)	0.1 (0.1)	0.1 (0.1)
Center of initial wavepacket (R_0)	7	10	10	11.5	10
Width of the wavepacket α	8	6	6	8	6
Smoothing of the wavepacket β	0.2	0.5	0.5	0.2	0.5
Initial translational energy (eV)	0.03, 0.08, 0.35 0.45, 0.75	0.05, 0.1, 0.2, 0.3, 0.4, 0.6, 0.8, 1.0	0.05, 0.2, 0.4, 0.6, 0.8, 1.0	0.03, 0.08, 0.35 0.45, 0.75	0.7
Analysis line R_∞	10	10	10	10	10

II. RESULTS AND DISCUSSION

The method employed for the calculations is the real wavepacket approach by Gray and Balint-Kurti,[35] in product coordinates so as to permit the computation of state-to-state reaction probabilities. The method has been well documented in the literature, and the reader is referred to the literature for further details.[35–37]

All parameters used in the calculations are listed in Table I. Each product arrangement channel for each electronic state requires a separate calculations. Results for energies in the range of 0.1–1.1 eV total energy (translational energy +initial state energy) are presented. To cover this energy range, several calculations with varying initial translational energies had to be carried out, as shown in Table I.

Figure 1 shows the reaction probabilities on the ground state PES for both product arrangement channels as well as the total reaction probability. The OH+Cl channel is preferred for all the energies considered here. The OH+Cl probability jumps to almost unity even for near zero collision energies. Around 0.5 eV total energy, the magnitude begins to decrease. The probability is dominated by a rich structure, especially in the low energy region. The reaction probability levels off at around 0.3 for energies above 0.65 eV.

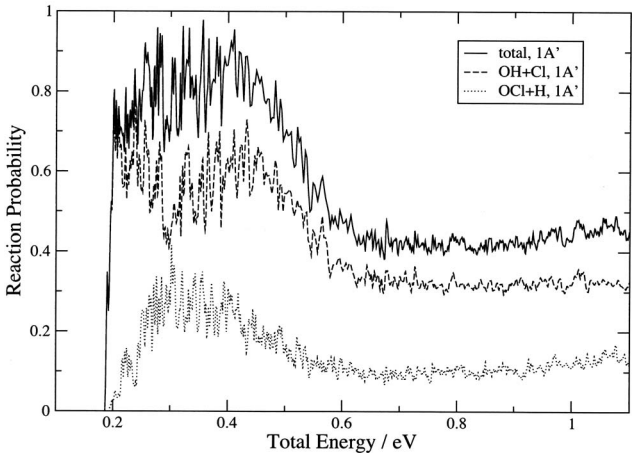

FIG. 1. The figure shows the reaction probabilities vs total energy in eV for the OH+Cl and OCl+H product arrangement channel obtained on the ground state surface, $1\,^1A'$. Also shown is the total reaction probability.

The reaction probability for the OCl+H channel rises steadily between 0.2 and 0.3 eV and then starts to decrease. This behavior differs markedly from that of the OH channel. The reaction probability for the OCl+H channel is smaller than that for OH+Cl for all energies shown. The OCl+H probability also shows a rich structure but not as narrow and pronounced as in the case of the OH+Cl channel. As for the production of OH, the OCl+H reaction probability becomes independent of energy above 0.65 eV.

The overall picture is similar to that obtained for the first generation PES using a time-independent method.[29] The total reaction probability displays a rich structure and is between 0.8 and 1.0 for energies below 0.5 eV but then decreases before leveling off at around 0.65 eV. The OH+Cl channel is preferred over the OCl+H channel for all energies. On the first generation PES, the OCl+H reaction probability jumps to around 0.3 for near zero collision energies, while in the new results, the rise is more gradual. Both product channel reaction probabilities are smaller than the first generation PES results for energies above 0.5 eV.

Figure 2 shows the reaction probabilities for the two excited states, $1A''$ and $2A'$. The reaction probability for the OH+Cl channel on the $1A''$ state PES rises steadily with energy but then decreases again for energies above 1.0 eV. For this state, the reaction probability shows hardly any structure apart from the very low energy region. The probability shows several broad peaks above 0.5 eV. The results on the first generation PES showed a more rapid rise in magnitude above the threshold and the earlier results are much larger in magnitude for energies between 0.3 and 0.7 eV. The earlier results also displayed less structure.

The probability for the OCl+H channel is zero below 0.7 eV. Above this energy, the probability rises rapidly displaying three broad structures. In contrast to the ground state, the reaction probability for the OCl+H channel is larger than the one for the OH+Cl channel above 0.75 eV. This behavior is also different from that found in the previous calculations on the first generation PES.[29] The earlier results

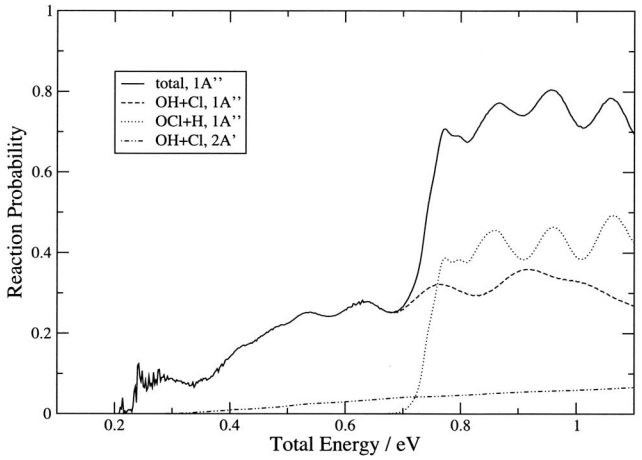

FIG. 2. The figure shows the reaction probabilities vs total energy in eV for the OH+Cl and OCl+H product arrangement channel obtained on the two excited states, $1A''$ and $2A'$. Also shown is the total reaction probability for the $1A''$ state.

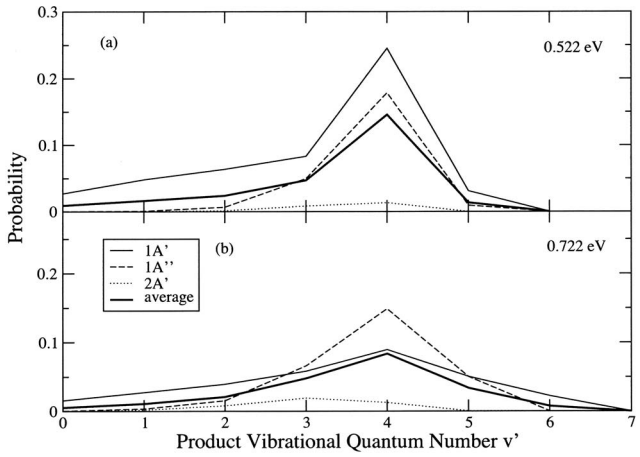

FIG. 3. The figure shows the vibrational distributions for the OH+Cl product arrangement channel at the total energies of (a) 0.522 and (b) 0.722 eV (7.6 and 12.2 kcal/mol collision energies) for all three electronic states (legend is the same for both panels).

showed the OCl+H $1A''$ probability much lower than the one for the OH+Cl channel for energies below 0.85 eV (results for an energy range from 0.15 to 0.85 eV were presented). This is due to a shift of the threshold for reaction to lower energies by about 0.1 eV from ≈0.8 to ≈0.7 eV of the current results, which is a result of the lower barrier height, by 0.08 eV on the new improved PES employed here. Also, the increase in magnitude with energy above the threshold is more rapid for the current results. In the current work, due to the magnitude and the shift in energy, one would expect that the $1A''$ probability contributes significantly to the overall OCl+H reaction probability above 0.7 eV.

Also shown is the reaction probability for the OH+Cl channel on the $2A'$ surface. This probability is much smaller in magnitude than the other ones. The probability is smooth, showing no structures, and rises linearly for the whole energy range shown. This behavior is similar to the first generation PES but the current results are much larger than the earlier ones.

Figure 3 shows the product vibrational state distributions for the OH+Cl channel and all three electronic states for two collision energies, 7.6 kcal/mol (0.522 eV total energy) and 12.2 kcal/mol (0.722 eV total energy). Figure 3(a) shows the vibrational distributions for the OH+Cl channel for all three electronic states at a total energy of 0.522 eV. For all three electronic states, the general picture is the same. The vibrational distributions are inverted peaking at $v'=4$. Also shown are the average distributions over all three electronic states which also peak at $v'=4$.

Figure 3(b) shows the same distributions as Fig. 3(a) but for a total energy of 0.722 eV. The general picture is the same as for the lower energy. For all three electronic states higher vibrational levels are favored. The distribution for the $1A'$ state vibrational levels peaks at $v'=4$ but with lower vibrational levels, having a higher population than for the lower energy. The $1A''$ state distribution has a pronounced peak at $v'=4$, while the $2A'$ distribution peaks at $v'=3$. The average distribution peaks at $v'=4$.

Figure 4(a) shows the vibrational distribution for the OCl+H channel on the ground state PES at a total energy of 0.522 eV. Due to the large threshold for this product arrangement channel on the $1A''$ surface, the contribution at the energy chosen is zero and the $2A'$ surface does not correlate to the OCl+H products. For this product arrangement channel, the vibrational distribution peaks at $v'=0$ with a second smaller peak at $v'=2$. The probability for producing vibrational level $v'=4$ and above is zero. This behavior is very different from the one observed for the OH+Cl channel.

Figure 4(b) shows the OCl+H product channel vibrational state distributions for the $1A'$ and $1A''$ electronic states at a total energy of 0.722 eV. The vibrational level distribution for the $1A'$ state is nearly flat. The distribution for the $1A''$ state shows the highest population for $v'=0$ and 1 with the population decreasing rapidly for higher vibrational states. The average vibrational level distribution of both electronic states is nearly flat with the population for $v'=6$ and above being zero.

The results for OCl+H channel are similar to the results from the first generation PES. For the OH+Cl channel, the

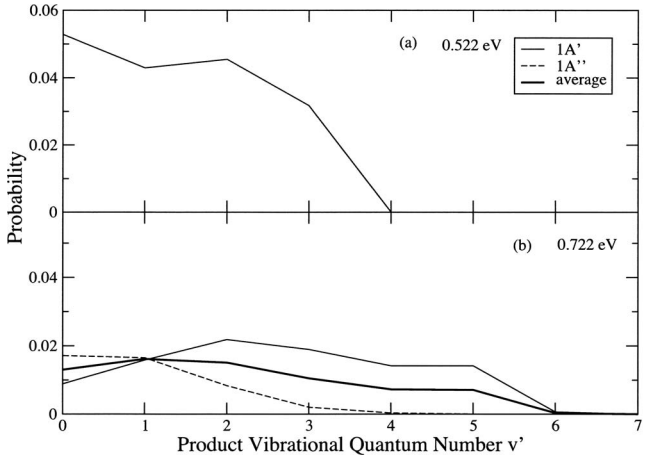

FIG. 4. The figure shows the vibrational distributions for the OCl+H product arrangement channel at the total energies of (a) 0.522 and (b) 0.722 eV (7.6 and 12.2 kcal/mol collision energies) for the two contributing electronic states (legend is the same for both panels).

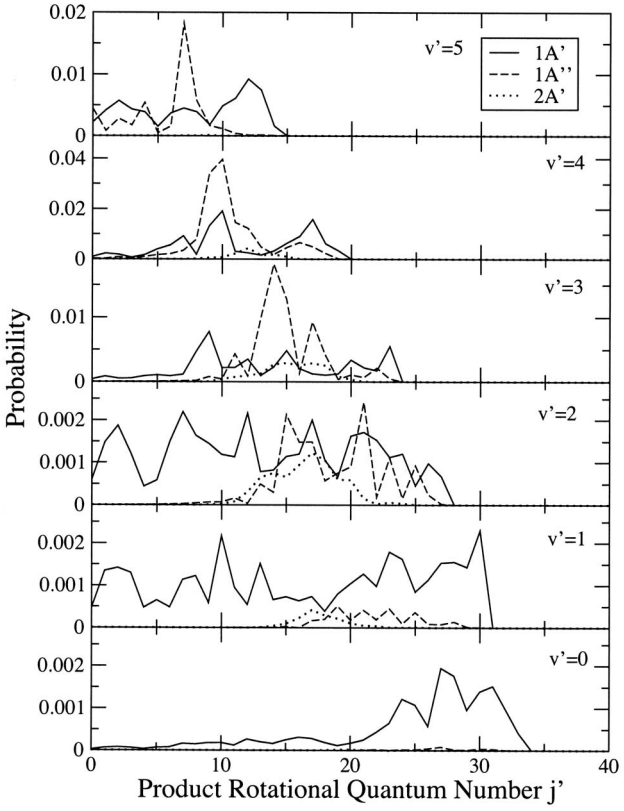

FIG. 5. The figure shows the rotational distributions for the OH+Cl product arrangement channel (averaged over an energy window of 0.65–0.75 eV total energy) for all three electronic states. Distributions for the first six product vibrational states, $v'=0-5$, are shown (legend is the same for all panels).

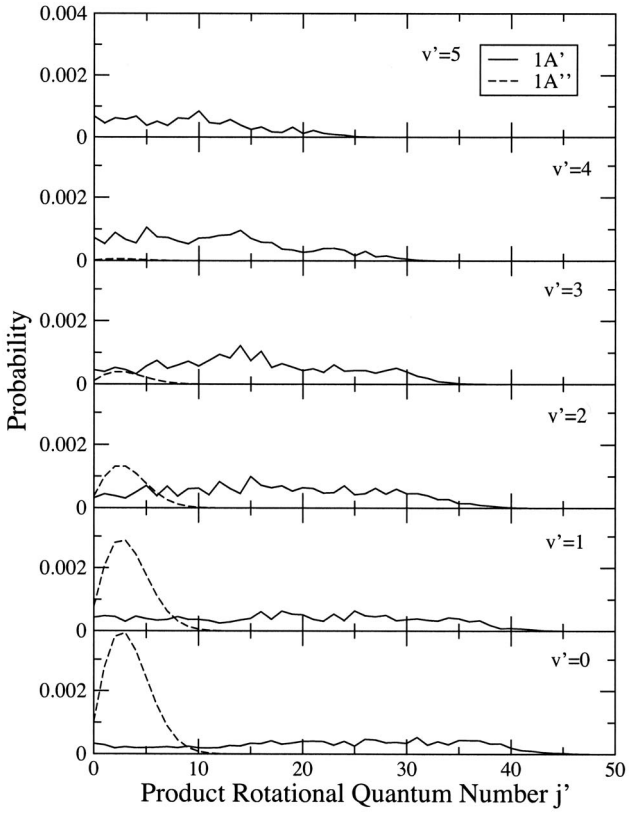

FIG. 6. The figure shows the rotational distributions for the OCl+H product arrangement channel (averaged over an energy window of 0.65–0.75 eV total energy) for both contributing electronic states. Distributions for the first six product vibrational states, $v'=0-5$, are shown (legend is the same for all panels).

results from the two excited electronic states confirm the results from the first generation PES. On the ground electronic states, the peak at $v'=4$ is more pronounced in the current results. Reference 28 also shows vibrational distributions at 0.449 eV for the $1A'$ state averaged over several initial rotational states which, while peaking at $v'=4$, show no pronounced peak. Preliminary calculations on the new $1A'$ PES show that averaging over initial rotational states is likely to have no significant effect on the $1A'$ OH vibrational distribution with the average still displaying a pronounced peak at $v'=4$.

Figures 5 and 6 show the product rotational state distributions for both channels and all three electronic states. The distributions present an average over an energy window from 0.65 to 0.75 eV total energy. Distributions for the first six vibrational states are shown.

The OH+Cl distributions are shown in Fig. 5. (Note: The *y*-axis scaling is different for all vibrational states.) The distributions for the $1A'$ state are different for different vibrational states. For $v'=0$, rotational states between $j'=20$ and 35 are populated. For $v'=1,2$, rotational states up to $j'=30$ are more evenly populated. For $v'=3-5$, the distributions again show a similar behavior to $v'=0$ with the higher rotational states being more populated. The distributions for the $1A''$ and $2A'$ electronic states show a similar behavior. The distributions show that only the high rotational states are populated with the probability for the lower ones being zero. With increasing product vibrational quantum number, the distributions shift to lower rotational states.

The OCl+H rotational state distributions are shown in Fig. 6. (Note: The *y*-axis scaling is the same for all v'). The distributions for the $1A'$ are very similar for all six vibrational states. All accessible rotational states are populated. The distributions for the $1A''$ state are very different. They are smooth, like big blobs, and only the lowest rotational states are populated.

The results for both channels for the $1A'$ and $1A''$ electronic states are similar to the ones reported in Refs. 28 and 29. For the $2A'$ state, no comparison is possible as only distributions for an initially excited states have been reported.

III. CONCLUSIONS AND OUTLOOK

Reaction probabilities for the $O(^1D)+HCl$ reaction for both possible product arrangement channels and for total energies in the range from 0.1 to 1.1 eV have been presented. The calculations were performed using the global PESs by Nanbu *et al.*,[27] which include three electronic states, $1A'$, $2A'$, and $1A''$, and the time-dependent real wavepacket approach.[35] Individual product arrangement channel probabilities as well as total reaction probabilities have been presented. The reaction probabilities for the ground electronic state show a rich structure and the OH+Cl channel is pre-

ferred for the energy range considered. The reaction probabilities for the two excited electronic states are much smoother, showing hardly any structure. For the $1\,^1A''$ state, the OCl+H channel is preferred above the reaction threshold of 0.7 eV for this channel.

Product vibrational quantum state distributions were presented at two energies. The distributions for the OH+Cl channel at both energies are inverted peaking at $v'=3,4$ for all three electronic states. The distributions for OCl+H are flatter favoring the lower vibrational levels.

Product rotational distributions for both product arrangement channels and for all three electronic states were also presented. The OH distributions favor the higher rotational states, especially for the $1A''$ and $2A'$ electronic states. For OCl, the $1A'$ distributions are fairly flat and all possible rotational states are populated, while for the $1A''$ state, the distributions are smooth and only low rotational states are populated.

The present calculations differ from the earlier ones by Kamisaka *et al.*[28,29] with respect to the method used. The PES employed in the current study is also an improved version of the PES in Refs. 27–29, especially with regards to the HOCl equilibrium. The energy range covered in the current calculations is larger than in most previous quantum mechanical studies and was chosen to obtain results for OCl +H channel on the $1A''$ electronic state. The current results differ from the earlier ones for the $1A''$ electronic state for both product arrangement channel, showing different reaction thresholds and more structure in the probabilities. Our new results show that the $1A''$ electronic state is likely to contribute significantly to the dynamics of the production of OCl+H at 0.722 eV. For the OCl+H channel on the $1A'$ electronic state PES, different behavior is observed in the low energy region. The vibrational distributions for the OH +Cl channel on the $1A'$ surface reported here are different from those reported earlier with the current results showing a more pronounced peak at $v'=4$.

A manuscript giving a direct comparison between the new and the first generation PES by Nanbu is in preparation. The variation with energy of vibrational and rotational distributions for both product arrangement channel and the three electronic states will be presented. Calculations for excited initial vibrational and rotational states are in progress and will be presented in a separate study. We are also carrying out convergence tests to determine the smallest grid possible and lowest number of different initial translational energies to be used in $J>0$ calculations employing the DIFFREALWAVE code[38] to obtain state-to-state integral and differential cross sections for all three electronic states and both product arrangement channel.

ACKNOWLEDGMENTS

The calculations reported in this paper have been performed on the CMS computational facility housed by the Centre for Computational Molecular Science, Australian Institute for Bioengineering and Nanotechnology, University of Queensland, Australia. These computational facilities have been purchased from funds provided by the University of Queensland and the Queensland Smart State Research Facilities Fund. M.H. would like to thank Sun Microsystems and the University of Queensland for funding. H.Y. acknowledges financial support from The University of Queensland during a research visit to the Centre for Computational Molecular Science, April–July, 2007.

[1] A. C. Luntz, J. Chem. Phys. **73**, 5393 (1980).
[2] P. H. Wine, J. R. Wells, and A. R. Ravishankara, J. Chem. Phys. **84**, 1349 (1986).
[3] E. J. Kruus, B. I. Niefer, and J. J. Sloan, J. Chem. Phys. **88**, 985 (1988).
[4] C. R. Park and J. R. Wiesenfeld, Chem. Phys. Lett. **163**, 230 (1989).
[5] N. Balucani, L. Beneventi, P. Casavecchia, and G. G. Volpi, Chem. Phys. Lett. **180**, 34 (1991).
[6] Y. Matsumi, K. Tonokura, M. Kawasaki, K. Tsuji, and K. Obi, J. Chem. Phys. **98**, 8330 (1993).
[7] A. J. Alexander, M. Brouard, S. P. Rayner, and J. P. Simons, Chem. Phys. **207**, 215 (1996).
[8] Y. Matsumi and S. M. Shamsuddin, J. Chem. Phys. **103**, 4490 (1995).
[9] H. Kohguchi and T. Suzuki, ChemPhysChem **7**, 1250 (2006).
[10] R. Schinke, J. Chem. Phys. **80**, 5510 (1984).
[11] A. Laganà, G. Ochoa de Aspuru, and E. Gracia, J. Phys. Chem. **99**, 17139 (1995).
[12] M. L. Hernández, C. Redondo, A. Laganà, G. Ochoa de Aspuru, M. Rosi, and A. Sgamellotti, J. Chem. Phys. **105**, 2710 (1996).
[13] S. Skokov, K. A. Peterson, and J. M. Bowman, J. Chem. Phys. **109**, 2662 (1998).
[14] J. M. Alvariño, A. Bolloni, M. L. Hernández, and A. Laganà, J. Phys. Chem. A **102**, 10199 (1998).
[15] S. Skokov, J. Qi, J. M. Bowman, C.-Y. Yang, S. K. Gray, K. A. Peterson, and V. A. Mandelshtam, J. Chem. Phys. **109**, 10273 (1998).
[16] J. M. Alvariño, A. Rodríguez, A. Laganà, and M. L. Hernández, Chem. Phys. Lett. **313**, 199 (1999).
[17] K. A. Peterson, S. Skokov, and J. M. Bowman, J. Chem. Phys. **111**, 7446 (1999).
[18] K. M. Christoffel, Y. Kim, S. Skokov, J. M. Bowman, and S. K. Gray, Chem. Phys. Lett. **315**, 275 (1999).
[19] T. Matínez, M. L. Hernández, J. M. Alvariño, A. Laganà, F. J. Aoiz, M. Menéndez, and E. Verdasco, Phys. Chem. Chem. Phys. **2**, 589 (2000).
[20] S. Y. Lin, K.-L. Han, and J. Z. H. Zhang, Phys. Chem. Chem. Phys. **2**, 2529 (2000).
[21] S. Y. Lin, K.-L. Han, and J. Z. H. Zhang, Chem. Phys. Lett. **324**, 122 (2000).
[22] M. Bittererová and J. M. Bowman, J. Chem. Phys. **113**, 1 (2000).
[23] M. Bittererová, J. M. Bowman, and K. Peterson, J. Chem. Phys. **113**, 6186 (2000).
[24] V. Piermarini, G. G. Balint-Kurti, S. K. Gray, F. Göğtas, A. Laganà, and M. L. Hernández, J. Phys. Chem. A **105**, 5743 (2001).
[25] V. Piermarini, A. Laganà, and G. G. Balint-Kurti, Phys. Chem. Chem. Phys. **3**, 4515 (2001).
[26] K. M. Christoffel and J. M. Bowman, J. Chem. Phys. **116**, 4842 (2002).
[27] S. Nanbu, M. Aoyagi, H. Kamisaka, H. Nakamura, W. Bian, and K. Tanaka, J. Theor. Comput. Chem. **1**, 263 (2002).
[28] H. Kamisaka, H. Nakamura, S. Nanbu, M. Aoyagi, W. Bian, and K. Tanaka, J. Theor. Comput. Chem. **1**, 275 (2002).
[29] H. Kamisaka, H. Nakamura, S. Nanbu, M. Aoyagi, W. Bian, and K. Tanaka, J. Theor. Comput. Chem. **1**, 285 (2002).
[30] S. Y. Lin and S. C. Park, Bull. Korean Chem. Soc. **23**, 229 (2002).
[31] F. Göğtas, N. Bulut, and S. Akpinar, J. Mol. Struct. **625**, 177 (2003).
[32] T. Martínez, M. L. Hernández, J. M. Alvariño, F. J. Aoiz, and V. Sáez Rábanos, J. Chem. Phys. **119**, 7871 (2003).
[33] W. Bian and B. Poirier, J. Chem. Phys. **121**, 4467 (2004).
[34] S. Nanbu (unpublished).
[35] S. K. Gray and G. G. Balint-Kurti, J. Chem. Phys. **108**, 950 (1998).
[36] M. Hankel, G. G. Balint-Kurti, and S. K. Gray, J. Chem. Phys. **113**, 9658 (2000).
[37] M. Hankel, G. G. Balint-Kurti, and S. K. Gray, J. Phys. Chem. **105**, 2330 (2001).
[38] M. Hankel, S. C. Smith, R. J. Allan, S. K. Gray, and G. G. Balint-Kurti, J. Chem. Phys. **125**, 164303 (2006).